Dalton Transactions

PAPER

View Article Online
View Journal | View Issue

Cite this: *Dalton Trans.*, 2014, **43**, 9356

Labile coordination approach for the modulation of the electronic properties of ruthenium(II) and iridium(III) complexes within an "N-heterocyclic carbene (NHC)–pyridyl" dynamic platform†

Moumita Mondal,‡ T. K. Ranjeesh,‡ Suraj K. Gupta and Joyanta Choudhury*

Received 21st February 2014,
Accepted 17th March 2014

DOI: 10.1039/c4dt00551a

www.rsc.org/dalton

Modulating the functionality of a synthetic transition metal complex by external stimuli is highly important for designing switchable systems. One prerequisite for achieving such dynamic activity is to generate molecular systems with *in situ* controllable electronic properties. To achieve dynamic control of the electronic properties, here we report the synthesis of two new N-heterocyclic carbene (NHC)–pyridyl Ir^{III}/Ir^{III} (**3**) and Ru^{II}/Ru^{II} (**4**) bimetallic complexes. These complexes include a latent stimuli-responsive labile site. This is utilized successfully for the on-demand, real-time modulation of the electronic properties of the systems in a reversible manner using external agents, as probed by spectroscopic and electrochemical techniques. These results display promising scope in the domain of transition metal–NHC chemistry, which can guide us in developing future smart organometallic systems.

Introduction

Bifunctionality of a molecule is a highly desirable property in view of designing smart and modular systems in catalysis, materials, and many other applications.[1] This is simply because one can regulate the property of one function by modifying the other in a single molecule. However, a serious limitation of having two fixed/static functional units is the lack of on-demand control and/or switching of a given property. One attractive alternative approach involves the addition of a dynamic functional unit, whose influence can be modulated by applying external stimuli (*e.g.*, coordination environment, light, redox, pH). Thus one can envision a stimuli-controllable bifunctional architecture within a single molecule. This would enable the on-demand, real-time tuning of a property and avoid the synthesis of an array of various static bifunctional molecules. The enormous success of N-heterocyclic carbene (NHC) ligands recently has prompted coordination and organometallic chemists to design and develop interesting tunable scaffolds in the domains of catalysis and materials.[2] Specifically, biscarbene ligands have been reported which incorporate the same or different metal precursors to achieve tandem reactions,[3] and these can be used in various elegant photophysical/materials applications.[4] Stimuli-active NHC ligands[5] and stimuli-switchable catalysis by NHC complexes,[6] recently introduced by Bielawski, Lavigne, Glorius, Plenio, Schanz and others, are receiving growing attention in this field.

In this context, we have focused our research on exploring an exciting opportunity to develop NHC–pyridyl-based heteroditopic ligands[7] for applying a dynamic platform (Fig. 1) for the *in situ* modification of electronic properties. We expect that the pyridyl-based unit would be utilized to operate stimuli-triggered (*e.g.*, coordination environment, light, redox, pH) functional changes which could induce the tuning of the electronic properties of the NHC-based complexes. A dynamic, reversible stimuli-responsiveness at the pyridine site *via* a labile coordination approach, would thus form the basis of designing switchable materials with variable electronic properties.

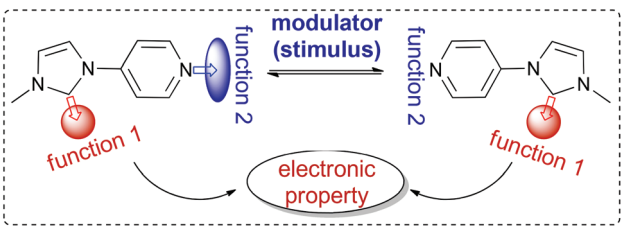

Fig. 1 Pictorial diagram of the NHC–pyridyl-based dynamic platform.

Organometallics & Smart Materials Laboratory, Department of Chemistry, Indian Institute of Science Education and Research Bhopal, Bhauri, Indore By-pass Road, Bhopal 462 066, India. E-mail: joyanta@iiserb.ac.in

†Electronic supplementary information (ESI) available: NMR and ESI-HR mass spectra; crystallographic details; stimuli-responsive studies; electrochemical details and DPV plots; additional ESI-HR mass spectra and figures. CCDC 945722 and 945723. For ESI and crystallographic data in CIF or other electronic format see DOI: 10.1039/c4dt00551a

‡M.M. and R.T.K. contributed equally.

Herein, we report the experimental execution of the above approach by interlinking non-symmetric "M–NHC"/"M–pyridine" (M = Ir^{III}, Ru^{II}) centers within a heteroditopic NHC–pyridyl ligand scaffold, through orthogonal cyclometalation and coordination strategies. An on-demand (chemical) stimuli-controlled reversible modulation of the electronic properties of the functional Ir^{III} and Ru^{II} complexes has been demonstrated in this report, which can be considered as a prerequisite for potential switchable systems based on transition metal–NHC complexes.

Results and discussion

The non-symmetric NHC–pyridyl Ir^{III}/Ir^{III} and Ru^{II}/Ru^{II} homobimetallic complexes, $[ClCp^*Ir^{III}(\mu\text{-PyIm})Ir^{III}Cp^*Cl_2]$ (**3**) and $[Cl(p\text{-cym})Ru^{II}(\mu\text{-PyIm})Ru^{II}(p\text{-cym})Cl_2]$ (**4**) (Cp* = pentamethylcyclopentadienyl, C_5Me_5; *p*-cym = *para*-cymene), were synthesized from the imidazolium salt $[PyImH_2]^+Cl^-$ (**1**) *via* a one-step transmetalation reaction with Ag_2O and an orthogonal complexation reaction with the Ir^{III} or Ru^{II} precursors (Scheme 1). The reaction of 1-(4-pyridyl)-3-methyl imidazolium chloride, $[PyImH_2]^+Cl^-$(**1**) with 0.55 equiv. of Ag_2O in dry dichloromethane, and the subsequent addition of 1 equiv. of a half-sandwich dimer, $[Cp^*IrCl_2]_2$ or $[(p\text{-cym})RuCl_2]_2$, resulted in the selective formation of **3** and **4** respectively in excellent yields. We did not get monometallic cyclometalated complexes (free of pyridine coordination) when 0.5 equiv. of the half-sandwich Ir or Ru dimer was used. It is worth mentioning here that the intermediate transmetalating silver carbene complex **2** was isolated from an independent reaction of **1** with Ag_2O in a mixture of dry CH_2Cl_2–CH_3OH (1 : 1) at ambient temperature, and it was also found to react efficiently with the iridium and ruthenium precursors to generate **3** and **4** respectively (Scheme 1).

Coordination of the N-heterocyclic carbene center to iridium or ruthenium was accompanied by an intramolecular aromatic C–H bond activation at the pyridine ring to afford the five-membered cyclometalated $Ir^{III}(C_{carbene}\text{^}C_{pyridyl})$ and $Ru^{II}(C_{carbene}\text{^}C_{pyridyl})$ cores in **3** and **4** respectively. In addition, an orthogonal coordination of the "Cp^*IrCl_2" or "(*p*-cym)-$RuCl_2$" unit to the pendant pyridyl ligand site occurred simultaneously, to generate a non-symmetric homobimetallic environment in both complexes. These new Ir^{III}/Ir^{III} (**3**) and Ru^{II}/Ru^{II} (**4**) complexes were characterized by ^1H and $^{13}C\{^1H\}$ NMR spectroscopy, electrospray ionization mass spectroscopy (ESI-MS) and single-crystal X-ray diffraction analyses. In the ^1H NMR spectra of **3** and **4**, the absence of an imidazolium C–H signal, and the appearance of three distinct signals for the pyridyl ring, provided evidence in favor of the cyclometalated $Ir^{III}(C_{carbene}\text{^}C_{pyridyl})$ and $Ru^{II}(C_{carbene}\text{^}C_{pyridyl})$ motifs featuring a loss of symmetry of the pyridyl ring. In $CDCl_3$, these three pyridyl proton signals appeared with an integration ratio of 1 : 1 : 1 at 9.03, 8.49, and 7.05 ppm in the case of **3**, and at 9.52, 8.52, and 6.91 ppm in the case of **4**. On the other hand, the intermediate monodentate carbene-coordinated silver complex **2** displayed a multiplet and a doublet of doublets (with an integration ratio of 2 : 2) at 8.69 and 7.87 ppm respectively, as expected due to the free non-cyclometalated symmetric pyridyl ring. Also, there were signatures present for two different types of Cp* and *para*-cymene resonances, also indicating the non-symmetric Ir^{III}/Ir^{III} and Ru^{II}/Ru^{II} environments in **3** and **4**, respectively. The $^{13}C\{^1H\}$ NMR spectra of **3** and **4** showed the characteristic metal–$\boldsymbol{C}_{carbene}$ and metal–$\boldsymbol{C}_{pyridyl}$ signals at 169.4 and 154.5 ppm and 192.5 and 157.7 ppm respectively. The Ir^{III}/Ir^{III} (in **3**) and Ru^{II}/Ru^{II} (in **4**) bimetallic architecture was confirmed by positive ion electrospray ionization mass spectrometry (ESI-MS) with a major intense peak at m/z = 884.1704 (**3**) and m/z = 700.0400 (**4**) assigned to $[M - Cl]^+$. Moreover, HRMS analyses of **3** and **4** supported the proposed structures based on a good agreement between the experimentally obtained and theoretical spectra (see ESI†).

The proposed non-symmetric homobimetallic structural arrangements in **3** and **4** based on NMR and mass spectroscopy results were unambiguously confirmed by X-ray diffraction studies. The molecular structure of **3** (Fig. 2) consisted of one "$Cp^*Ir^{III}Cl$" fragment (Ir1) and one "$Cp^*Ir^{III}Cl_2$" (Ir2) interconnected by the NHC–pyridyl ligand through a heteroditopic coordination mode. The NHC-coordination, along with cyclometalation of the pyridyl ring in the ligand, led to the formation of a five-membered chelate around the iridium center (Ir1) with a $C_{carbene}$–Ir^{III}–$C_{pyridine}$ bite angle of 79.47(9)°, and Ir^{III}–$C_{carbene}$ and Ir^{III}–$C_{pyridine}$ bond distances of 2.0463(4) Å and 2.064(4) Å, respectively. The characteristic three legged

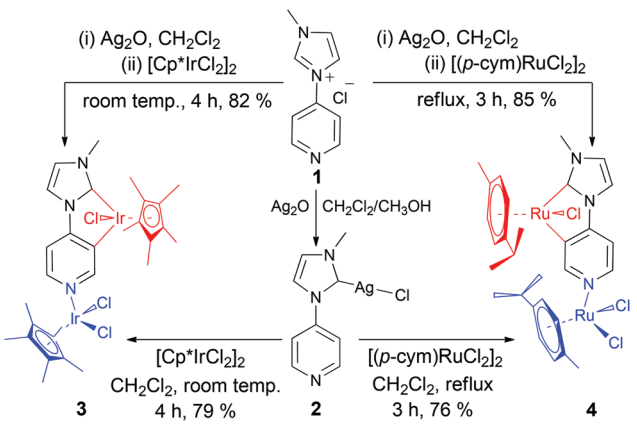

Scheme 1 Synthesis of **3** and **4**.

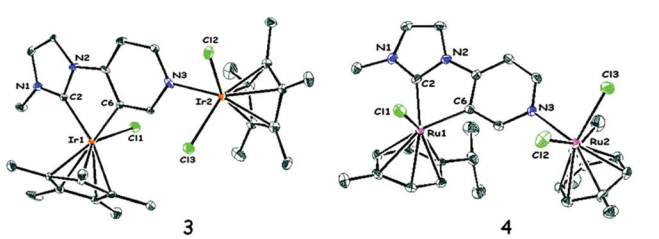

Fig. 2 X-ray crystal structures of **3** and **4**.[8] Thermal ellipsoids are at a 30% probability level. Hydrogen atoms are omitted for clarity.

piano-stool arrangement around the other iridium center (Ir2) could be viewed with the pyridine and two chloro ligands as the legs and a Cp* ring as the seat, tethered by the metal atom. The Ir^{III}–$N_{pyridine}$ bond distance was 2.069(11) Å. The structure of **4** (Fig. 2) was similar to that of **3**. The $C_{carbene}$–Ru^{II}–$C_{pyridine}$ bite angle was 76.76(16)°, whereas the Ru^{II}–$C_{carbene}$ and Ru^{II}–$C_{pyridine}$ bond distances were 2.016(4) Å and 2.067(4) Å, respectively, around the chelated ruthenium (Ru1) center. The intermetallic through-space distances in **3** and **4** were 6.008 Å (Ir···Ir) and 6.106 Å (Ru···Ru), respectively, which are considered as optimum distances required for a possible metal–metal cooperative communication.[9]

As we explained earlier, the reversible modulation and fine-tuning of the electronic properties of metal–NHC complexes is of growing interest in recent times. Regarding our systems, we investigated the feasibility of remote switching the decoordination–recoordination of the transition metal centers at the pyridine site, to modify the coordination environment and hence the electronic effect. An illustration of the proposed dynamic modification experiments with the representative ruthenium complex **4** is detailed herein (Scheme 2, Fig. 3).

Gratifyingly, the addition of 1 equiv. of PPh_3 to a $CDCl_3$ solution of **4** resulted in significant upfield shifts for the pyridyl *ortho* protons (labelled as ■, ▲) as well as the imidazole backbone protons (labeled as ●) of the NHC–pyridyl scaffold, as monitored by ^1H NMR spectroscopy (Fig. 3A(b) and Scheme 2). This observation was presumably due to the decoordination of the "(*p*-cym)$RuCl_2$" (a Ru^{II}-d^6 ML_3X_2 fragment) site in **4** with the stronger PPh_3 ligand, generating $[Ru^{II}(p\text{-cym})(PPh_3)Cl_2]$[10] and the decoordinated complex **5**. This consequence reflected the pronounced effect of Ru^{II}-pyridine coordination in **4**, inducing a substantial electron-deficiency in the system. **4** could comfortably be regenerated *via* the addition of $[(p\text{-cym})RuCl_2]_2$ to the reaction mixture (Fig. 3A(c) and Scheme 2). The recoordination of different metal centers with variable electronic influences and coordination environments, *e.g.*, "IrCp*Cl_2" (a Ir^{III}-d^6 ML_2X_3 fragment) to the open pyridine-site in the decoordinated complex **5**, was also proved by observing different degrees of downfield shift of the ^1H NMR signals for the relevant protons in the mixed-metal system **7** (Fig. 3A(d) and Scheme 2). The above insight prompted us to envision a reversible switching of electronic properties upon protonation–deprotonation of the decoordinated system **5**. Thus, the addition of CF_3COOH to the decoordinated ruthenium complex **5** caused downfield shifts for the pyridyl protons (labelled as ▲, ◆) as well as the imidazole backbone protons (labeled as ●) of the NHC–pyridyl scaffold, due to the formation of protonated species **6** (Fig. 3B(e) and Scheme 2). Complex **6** may be considered as a system with a pyridin-3-ylidene/imidazol-2-ylidene-based ligand.[7a–c,f,g] Advantageously, complex **5** was recovered through the addition of NEt_3 to the above solution (Fig. 3B(f) and Scheme 2). To complete the cycle, **4** was regenerated again through the addition of $[(p\text{-cym})RuCl_2]_2$ to a solution containing the deprotonated species (Fig. 3B(g) and Scheme 2). Notably, the Ir^{III}/Ir^{III} complex **3** was also shown to be an equally efficient system for a similar type of coordination–decoordination and acid–base dependent modulation behavior (see ESI,† Fig. S22). $^{13}C\{^1H\}$ NMR spectroscopic analyses also highlighted a similar outcome of the electronic effects within the ligand system (Fig. 4A; M = Ir in a–d; M = Ru in e–h).

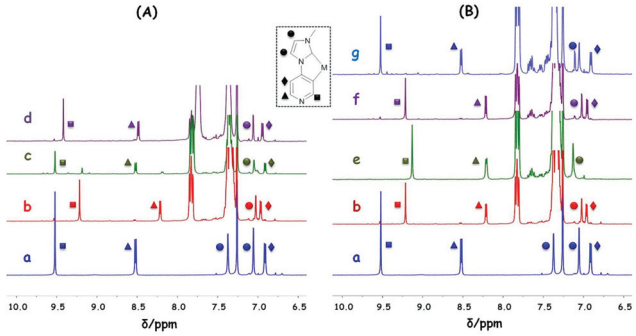

Fig. 3 Partial ^1H NMR spectra (400 MHz, $CDCl_3$, 300 K) for stimuli-controlled reversible decoordination–recoordination (A) and protonation–deprotonation (B) switching processes, demonstrated with [Cl(*p*-cym)Ru^{II}(μ-Pyim)Ru^{II}(*p*-cym)Cl_2] (**4**) (*vide* Scheme 2). (A) (a) **4** (starting); (b) **4** + PPh_3; (c) regenerated **4** (*via* **4** + PPh_3 + $[Ru(p\text{-cym})Cl_2]_2$); (d) **4** + PPh_3 + $[IrCp^*Cl_2]_2$. (B) (a) complex **4** (starting); (b) **4** + PPh_3; (e) **4** + PPh_3 + CF_3COOH; (f) **4** + PPh_3 + CF_3COOH + NEt_3; (g) regenerated **4** (via **4** + PPh_3 + CF_3COOH + NEt_3 + $[Ru(p\text{-cym})Cl_2]_2$). The residual solvent peak at δ = 7.26 ppm in $CDCl_3$ was taken as a reference for all the spectra. The relevant protons in the complex backbone have been labelled (as ■, ▲, ◆, and ● on the structure) and shown in the figure. Generation of the decoordinated/recoordinated and protonated/deprotonated species was confirmed by the isolation and characterization of the corresponding ruthenium complexes **5**, **6**, and **7** independently, as well as by recording ESI-HRMS data in solution (see Experimental section and ESI†).

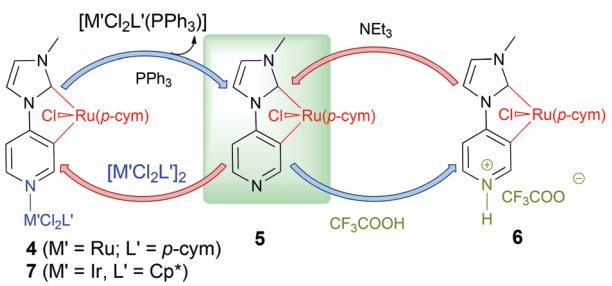

Scheme 2 Proposed *in situ* stimuli-controlled reversible decoordination–recoordination and protonation–deprotonation switching processes with **4**.

The above-observed reversible NMR chemical shifts of only the protons and carbons of the ligand backbone might not be reliable as stand-alone evidence for the modulation or switching of the electronic properties of the supporting NHC-ligand in **3** and **4**. Therefore, to further evaluate the reversible, stimuli-controlled electronic perturbation at the cyclometalated "M($C_{carbene}$^$C_{pyridyl}$)" center, we used electrochemical methods, which are rather reliable and sensitive as a probe. The half-wave potential ($E_{1/2}$) values derived from differential pulse voltammetry (DPV) of the Ir^{III}/Ir^{IV} (in a–d) and Ru^{II}/Ru^{III}

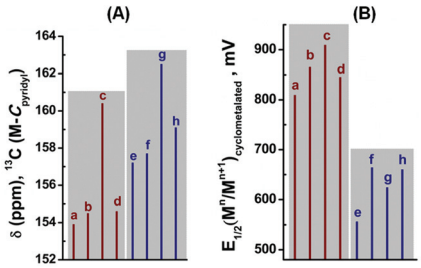

Fig. 4 (A) $^{13}C\{^1H\}$ NMR (100 MHz, $CDCl_3$, 300 K) chemical shift values (in ppm) of the "M–$C_{pyridyl}$" carbon atom and (B) $E_{1/2}$ values (in mV, *vs.* SCE) of the Ir^{III}/Ir^{IV} and Ru^{II}/Ru^{III} redox couples in a cyclometalated "LM($C_{carbene}$^$C_{pyridyl}$)Cl" motif: (a) **3** + PPh_3; (b) **3** (starting); (c) **3** + PPh_3 + CF_3COOH; (d) **3** + PPh_3 + $[Ru(p\text{-cym})Cl_2]_2$; (e) **4** + PPh_3; (f) **4** (starting); (g) **4** + PPh_3 + CF_3COOH; (h) **4** + PPh_3 + $[IrCp^*Cl_2]_2$ (*vide* Scheme 2). Generation of the decoordinated–recoordinated and protonated–deprotonated species was confirmed by the isolation and characterization of the corresponding ruthenium complexes **5**, **6**, and **7** independently, as well as by recording ESI-HRMS data in solution (see Experimental section and the ESI†). Electrode potentials ($E_{1/2}$) were determined by differential pulse voltammetry (DPV) in dry CH_3CN. Ferrocene ($E_{1/2}$, Fc/Fc^+ = 401 mV) was used as the calibration standard. For details, see the ESI†.

(in e–h) redox couples are shown in Fig. 4B. For both the iridium and ruthenium systems, coordination and protonation at the remote pyridine site generated an electron-poor and less electron-donating cyclometalating ligand when compared to the decoordinated–deprotonated systems. This trend is evident from the higher Ir^{III}/Ir^{IV} and Ru^{II}/Ru^{III} oxidation potential values in the homo- and heterobimetallic complexes, as shown in b and d (by 56 mV and 36 mV) as well as in f and h (by 108 mV and 104 mV), compared to the decoordinated complexes shown in a and e respectively (Fig. 4B). The effect of protonation on the decoordinated complexes is also in line with the expected generation of a ligand backbone with less donating ability towards the metal center (the $E_{1/2}$ of the Ir^{III}/Ir^{IV} couple in the protonated complex (shown in c) is ~100 mV higher than in the free complex; the $E_{1/2}$ of the Ru^{II}/Ru^{III} couple in the protonated complex (shown in g) is ~70 mV higher than in the free complex).

Reversible repeatability of the decoordination–recoordination and protonation–deprotonation processes was confirmed in these systems by carrying out the steps several times successfully without substantial decomposition or any other side reactions. To validate all the above-described *in situ* phenomena, we isolated the representative decoordinated ruthenium complex **5** from the reaction of complex **4** with 1 equiv. of PPh_3 in chloroform at ambient temperature followed by chromatographic separation. Thereafter, we also isolated the protonated complex **6** by treating complex **5** with CF_3COOH, and the heterobimetallic complex **7** by treating it with $[IrCp^*Cl_2]_2$. The NMR spectroscopic, HR-ESIMS and electrochemical data obtained for the isolated complexes **5**, **6** and **7** were found to be identical with those observed for the *in situ* generated systems. A similar strategy to isolate the decoordinated iridium complex was not successful due to insufficient stability of the species during column chromatography. Nevertheless, we believe that the above experiments established a pronounced on-demand, reversible and controlled modulation of the electronic properties at an active center through a stimuli-sensitive remote site. Potential applicability of the above-developed phenomenon is currently being explored in our laboratory.

Conclusions

In summary, we have synthesized two new stimuli-active NHC–pyridyl Ir^{III}/Ir^{III} (**3**) and Ru^{II}/Ru^{II} (**4**) bifunctional complexes which respond successfully to reversible modulation of their electronic properties with external chemical agents. Both coordination and protonation at the remote pyridine site resulted in a reduced donating ability of the cyclometalated NHC ligand toward the metal center, generating an electron-deficient system. The original properties could be restored *via* a reverse process. These dynamic platforms exemplify a promising discovery in the domain of transition metal–NHC chemistry. We expect that the reversible decoordination–recoordination and protonation–deprotonation switching behavior of the complexes could potentially guide the development of stimuli-switchable materials.

Experimental section

General methods and materials

^1H and $^{13}C\{^1H\}$ NMR spectra were recorded on Bruker AVANCE III 400 MHz and 500 MHz NMR spectrometers. Chemical shifts (δ) are expressed in ppm using the residual proton resonance of the solvent as an internal standard ($CHCl_3$: δ = 7.26 ppm for the ^1H spectra, 77.2 ppm for the $^{13}C\{^1H\}$ spectra; DMSO: δ = 2.50 ppm for the ^1H spectra, 39.5 ppm for the $^{13}C\{^1H\}$ spectra). All coupling constants (J) are expressed in hertz (Hz) and are only given for ^1H–^1H couplings unless mentioned otherwise. The following abbreviations were used to indicate multiplicity: s (singlet), d (doublet), t (triplet), q (quartet), dd (doublet of doublets) and m (multiplet). ESI mass spectroscopy was performed on a Bruker microTOF QII spectrometer. UV-Vis spectra were recorded on a Perkin Elmer Lambda 25 spectrophotometer. Electrochemical experiments were done using a CHI 1120B Electrochemical Analyzer. Elemental analyses were performed with a Thermo Scientific FLASH 2000 elemental analyser at the Sophisticated Instrument Centre (SIC) in IIT Indore, India. Single-crystal X-ray diffraction data were collected using a Bruker SMART APEX II CCD diffractometer with graphite monochromated Mo Kα (λ = 0.71073 Å) radiation at 140 K. Dry solvents and reagents were obtained from commercial suppliers and used without further purification. Deuterated solvents were purchased from Aldrich. $IrCl_3{\cdot}xH_2O$ and $RuCl_3{\cdot}xH_2O$ were purchased from Johnson Matthey and used as received without further purification.

$[IrCp^*Cl_2]_2$ [11] and $[Ru(p\text{-cym})Cl_2]_2$ [12] were synthesized according to reported procedures.

Synthetic procedures

[1-(4-Pyridyl)-3-methyl]-imidazolium chloride, 1. *N*-Methyl imidazole (1.59 mL, 20 mmol) and 4-chloropyridine hydrochloride (1.5 g, 10 mmol) were mixed and stirred for 20 h at 90 °C in a pressure tube. After cooling, the formed solid was purified by repetitive precipitation from EtOH–Et_2O and the resulting product was dried *in vacuo*. Yield: 1.57 g (80%). ^{1}H NMR (400 MHz, [D$_6$]DMSO, 27 °C): δ = 10.19 (s, 1H, CH_{imz}), 8.87 (dd, J = 1.6 Hz, J = 4.6 Hz, 2H, CH_{pyr}), 8.51 (t, J = 1.9 Hz, 1H, CH_{imz}), 8.03–8.02 (m, 1H, CH_{imz}), 7.91 (dd, J = 1.6 Hz, J = 4.6 Hz, 2H, CH_{pyr}), 3.97 ppm (s, 3H, CH_{3imz}). ^{13}C{^{1}H} NMR (100 MHz, [D$_6$]DMSO, 27 °C): δ = 151.1, 142.0, 136.9, 125.0, 120.0, 115.4, 36.4 ppm. HRMS (ESI, positive ion): M^+ = 160.0894 (calculated as 160.0869 for $C_9H_{10}N_3^+$). Anal. Calc. for $C_9H_{10}N_3Cl{\cdot}0.25H_2O$: C, 54.01; H, 5.29; N, 20.99. Found: C, 53.98; H, 5.27; N, 21.23%.

Complex 2. Silver(I) oxide (64.0 mg, 0.275 mmol) was added to a suspension of **1** (98.0 mg, 0.5 mmol) in a mixture of CH_2Cl_2–MeOH (1 : 1) (15 mL) in a Schlenk tube. The reaction mixture was protected from light and stirred for 4 h at room temperature. After this period, the solution was filtered, and solvent was reduced to 3 mL under vacuum and then precipitated with Et_2O. The solid product was isolated by filtration and dried *in vacuo*. Yield: 75.0 mg (50%). ^{1}H NMR (400 MHz, [D$_6$]DMSO, 27 °C): δ = 8.70–8.69 (m, 2H, CH_{pyr}), 8.03 (d, J = 1.7 Hz, 1H, CH_{imz}), 7.87 (dd, J = 1.4 Hz, 4.7 Hz, 2H, CH_{pyr}), 7.78 (d, J = 1.7 Hz, 1H, CH_{imz}), 3.93 ppm (s, 3H, CH_{3imz}). ^{13}C{^{1}H} NMR (100 MHz, [D$_6$]DMSO, 27 °C): δ = 151.4, 146.2, 124.8, 121.5, 117.9, 38.8 ppm. N*C*N was not visible.[13] HRMS (ESI, positive ion): M^+ = 425.0676 (calculated 425.0638 for $[C_{18}H_{18}N_6Ag]^+$. The cation corresponds to $[Ag(NHC)_2]^+$ which is generated under ESI-MS conditions from [Ag(NHC)Cl]. A similar observation was reported earlier for this type of complex;[14] (ESI, negative ion): M^- = 178.8428 (calculated as 178.8415 for $[AgCl_2]^-$).

Complex 3. *Method A*: silver(I) oxide (25.4 mg, 0.11 mmol) was added to a suspension of **1** (39.1 mg, 0.2 mmol) in degassed CH_2Cl_2 (10 mL) in a Schlenk tube. The reaction mixture was protected from light and stirred for 2 h at room temperature under a nitrogen atmosphere. $[IrCp^*Cl_2]_2$ (79.6 mg, 0.1 mmol) was added to the resulting greyish brown suspension and the reaction mixture was stirred for 4 h at room temperature in the dark. The resulting solution was filtered through a celite plug. The bright yellow filtrate was reduced to a minimum volume under vacuum and the product was isolated by precipitating it with Et_2O, affording **3** as a yellow powder. Yield: 75.0 mg (82% based on the metal precursor). Recrystallization from CH_2Cl_2–Et_2O resulted in an analytically pure product. *Method B*: in a Schlenk tube, a mixture of $[IrCp^*Cl_2]_2$ (52.7 mg, 0.066 mmol) and **2** (20.0 mg, 0.066 mmol) in degassed CH_2Cl_2 (8 mL) was stirred for 4 h at room temperature under a nitrogen atmosphere in the dark. The reaction mixture was filtered through a celite plug. The bright yellow filtrate was reduced to a minimum volume under vacuum and the product was isolated by precipitating it with Et_2O, affording **3** as a yellow powder. Yield: 49.0 mg (80% based on the metal precursor). *Note*: Performing the reaction with a mixture of $[IrCp^*Cl_2]_2$ (39.5 mg, 0.04958 mmol) and **2** (30.0 mg, 0.099 mmol) under the same conditions yielded the complex **3** in a 79% yield (based on the metal precursor). ^{1}H NMR (400 MHz, $CDCl_3$, 27 °C): δ = 9.03 (s, 1H, CH_{pyr}), 8.49 (d, J = 6.0 Hz, 1H, CH_{pyr}), 7.40 (d, J = 1.9 Hz, 1H, CH_{imz}), 7.08 (d, J = 1.8 Hz, 1H, CH_{imz}), 7.05 (d, J = 6.0 Hz, 1H, CH_{pyr}), 4.01 (s, 3H, CH_{3imz}), 1.85 (s, 15H, CH_{3Cp^*}), 1.51 ppm (s, 15H, CH_{3Cp^*}). ^{13}C{^{1}H} NMR (100 MHz, $CDCl_3$, 27 °C): δ = 169.4, 160.3, 154.5, 147.5, 139.0, 123.2, 115.7, 107.0, 92.3, 85.6, 37.5, 10.3, 8.6 ppm. HRMS (ESI, positive ion): M^+ = 884.1704 (calculated 884.1690 for $[C_{29}H_{38}N_3Cl_2Ir_2]^+$). UV-Vis ($CH_2Cl_2$): λ_{max}/nm (ε/M^{-1} cm^{-1}): 229 (2.74×10^4), 288 (9.83×10^3). Anal. Calc. for $C_{29}H_{38}N_3Cl_3Ir_2$: C, 37.88; H, 4.16; N, 4.57. Found: C, 37.77; H, 4.16; N, 4.62%.

Complex 4. *Method A*: silver(I) oxide (25.4 mg, 0.11 mmol) was added to a suspension of **1** (39.1 mg, 0.2 mmol) in degassed CH_2Cl_2 (10 mL) in a Schlenk tube. The mixture was protected from light and stirred for 2 h at room temperature under a nitrogen atmosphere. $[Ru(p\text{-cym})Cl_2]_2$ (61.6 mg, 0.1 mmol) was added to the resulting greyish brown suspension and the reaction mixture was refluxed for 3 h in the dark. The resulting solution was cooled to room temperature and filtered through a celite plug. The brownish yellow filtrate was reduced to a minimum volume under vacuum and the product was isolated by precipitating it with Et_2O, affording **4** as a brownish yellow powder. Yield: 63.0 mg (85% based on the metal precursor). *Method B*: in a Schlenk tube, a mixture of $[Ru(p\text{-cym})Cl_2]_2$ (46.2 mg, 0.075 mmol) and **2** (22.6 mg, 0.075 mmol) in degassed CH_2Cl_2 (5 mL) was refluxed for 3 h under nitrogen atmosphere in the dark. The resulting solution was cooled to room temperature and filtered over a celite plug. The brownish yellow filtrate was reduced to a minimum volume under vacuum and the product was isolated by precipitating it with Et_2O, affording **4** as a brownish yellow powder. Yield: 44.0 mg (79% based on the metal precursor). *Note*: Performing the reaction with a mixture of $[Ru(p\text{-cym})Cl_2]_2$ (15.2 mg, 0.02475 mmol) and **2** (14.9 mg, 0.050 mmol) under the same conditions yielded the complex **4** in a 72% yield (based on the metal precursor). ^{1}H NMR (400 MHz, $CDCl_3$, 27 °C): δ = 9.52 (s, 1H, CH_{pyr}), 8.52 (d, 1H, J = 5.9 Hz, CH_{pyr}), 7.37 (d, 1H, J = 1.1 Hz, CH_{imz}), 7.06 (d, 1H, J = 1.2 Hz, CH_{imz}), 6.91 (d, 1H, J = 6.0 Hz, CH_{pyr}), 5.73–5.66 (m, 2H, C$H_{cym,\ aro}$), 5.63–5.59 (m, 2H, C$H_{cym,\ aro}$), 5.45–5.44 (m, 2H, C$H_{cym,\ aro}$), 5.24–5.21 (m, 2H, C$H_{cym,\ aro}$), 4.19 (s, 3H, CH_{3imz}), 3.04 (m, 1H, C*H*Me$_{2cym}$), 2.26 (m, 1H, C*H*Me$_{2cym}$), 2.12 (s, 3H, CH_{3cym}), 2.02 (s, 3H, CH_{3cym}), 1.35–1.32 (m, 6H, CH*Me*$_{2cym}$), 0.89 (d, J = 6.9 Hz, 3H, CH*Me*$_{2cym}$), 0.78 ppm (d, J = 6.9 Hz, 3H, CH*Me*$_{2cym}$). ^{13}C{^{1}H } NMR (100 MHz, $CDCl_3$, 27 °C): δ = 192.5, 164.6, 157.7, 153.7, 149.2, 123.6, 115.2, 107.0, 104.1, 103.3, 103.1, 97.1, 91.6, 90.3, 89.3, 86.3, 83.1, 82.7, 82.3, 82.2, 38.3, 31.2, 30.8, 23.4, 22.6, 22.4, 21.8, 19.2, 18.4 ppm. HRMS (ESI, positive ion): M^+ = 700.0400 (calculated as 700.0371 for $[C_{29}H_{36}N_3Cl_2Ru_2]^+$). UV-Vis

(CH_2Cl_2): λ_{max}/nm (ε/M^{-1} cm^{-1}): 231 (3.65×10^4), 294 (1.25×10^4). Anal. Calc. for $C_{29}H_{36}N_3Cl_3Ru_2{\cdot}0.5CH_2Cl_2$: C, 45.57; H, 4.80; N, 5.40. Found: C, 45.64; H, 4.86; N, 5.12%.

Complex 5. Complex **4** (8.8 mg, 11.88 μmol) was dissolved in $CHCl_3$ (2 mL) in a Schlenk tube and PPh_3 (4.6 mg, 17.54 μmol) was added to it. The resulting solution was stirred at room temperature for 1 h during which time the reaction was completed (as confirmed by ^{1}H NMR spectroscopy). The solvent was evaporated to yield a reddish solid residue which was then subjected to column chromatography on neutral alumina. Elution with CH_2Cl_2 afforded an orange solution corresponding to Ru(*p*-cym)$Cl_2(PPh_3)$. Complex **5** was eluted thereafter with CH_2Cl_2–MeOH (99 : 1 v/v). Evaporation of the solvent afforded pure complex **5** as a yellow solid. Yield: 3.1 mg (60%). ^{1}H NMR (400 MHz, $CDCl_3$, 27 °C): δ = 9.19 (s, 1H, CH_{pyr}), 8.21 (d, 1H, J = 5.3 Hz, CH_{pyr}), 7.39 (d, 1H, J = 1.8 Hz, CH_{imz}), 7.05 (d, 1H, J = 1.8 Hz, CH_{imz}), 7.03 (d, 1H, J = 5.3 Hz, CH_{pyr}), 5.71 (d, 1H, J = 6 Hz C$H_{cym,\ aro}$), 5.67 (d, 1H, J = 5.9 Hz C$H_{cym,\ aro}$), 5.63 (d, 1H, J = 5.9 Hz C$H_{cym,\ aro}$), 5.49 (d, 1H, J = 5.8 Hz C$H_{cym,\ aro}$), 4.19 (s, 3H, CH_{3imz}), 2.19 (m, 1H, CHMe$_{2cym}$), 2.09 (s, 3H, CH_{3cym}), 0.89 (d, 3H, J = 6.7 Hz, CHMe_{2cym}), 0.75 ppm (d, 3H, J = 6.9 Hz, CHMe_{2cym}). ^{13}C{^{1}H} NMR (100 MHz, $CDCl_3$, 27 °C): δ = 192.4, 160.6, 156.8. 152.6, 139.2, 124.7, 115.5, 107.5, 106.8, 102.0, 92.3, 91.0, 89.3, 85.9, 38.4, 31.3, 23.1, 21.9, 19.2 ppm. HRMS (ESI, positive ion): M^+ = 394.0833 (calculated as 394.0857 for $[C_{19}H_{22}N_3Ru]^+$). Anal. Calc. for $C_{19}H_{22}N_3ClRu{\cdot}CH_2Cl_2$: C, 46.75; H, 4.71; N, 8.18. Found: C, 46.68; H, 4.66; N, 8.11%.

Complex 6. To a $CDCl_3$ solution (0.4 mL) of isolated complex **5** (4.0 mg, 9.34 μmol), an equivalent amount of CF_3COOH (72 μL, 0.13 M solution in $CDCl_3$, ~9.34 μmol) was added. Complete formation of complex **6** was achieved after stirring for 1 h at an ambient temperature. Yield: quantitative. ^{1}H NMR (400 MHz, $CDCl_3$, 27 °C): δ = 9.16 (s, 1H, CH_{pyr}), 8.19 (d, 1H, J = 5.0 Hz, CH_{pyr}), 7.37 (broad s, 1H, CH_{imz}), 7.15 (d, 1H, J = 5.1 Hz, CH_{pyr}), 7.04 (broad s, 1H, CH_{imz}), 5.70 (d, 2H, J = 5.8 Hz C$H_{cym,\ aro}$), 5.65 (d, 1H, J = 6.0 Hz C$H_{cym,\ aro}$), 5.53 (d, 1H, J = 5.9 Hz C$H_{cym,\ aro}$), 4.21 (s, 3H, CH_{3imz}), 2.18 (m, 1H, CHMe$_{2cym}$), 2.09 (s, 3H, CH_{3cym}), 0.88 (d, 3H, J = 6.7 Hz, CHMe_{2cym}), 0.74 ppm (d, 3H, J = 6.9 Hz, CHMe_{2cym}). ^{13}C{^{1}H} NMR (100 MHz, $CDCl_3$, 27 °C): δ = 193.8, 163.1, 160.7 (q, $^2J_{CF}$ = 37 Hz, CF_3COO^-), 159.8, 148.9, 136.7, 125.6, 116.2 (q, $^1J_{CF}$ = 194 Hz, CF_3COO^-), 108.0, 107.8, 103.6, 92.6, 91.5, 90.3, 87.2, 38.6, 31.4, 23.0, 22.0, 19.2 ppm. (Note: one peak was not detected). ^{19}F{^{1}H} NMR (376 MHz, $CDCl_3$, 27 °C): δ = −75.8 ppm. HRMS (ESI, positive ion): M^+ = 430.0582 (calculated as 430.0620 for $[C_{19}H_{23}N_3ClRu]^+$). Elemental analysis of complex **6** could not be attempted due to its hygroscopic nature.

Complex 7. To a $CDCl_3$ solution (0.4 mL) of isolated complex **5** (4.0 mg, 9.34 μmol), $[IrCp^*Cl_2]_2$ (3.75 mg, 4.7 μmol) was added and stirred for 1 h at an ambient temperature to yield complex **7** in a quantitative yield. ^{1}H NMR (400 MHz, $CDCl_3$, 27 °C): δ = 9.42 (s, 1H, CH_{pyr}), 8.49 (d, 1H, J = 5.9 Hz, CH_{pyr}), 7.38 (d, 1H, J = 1.9 Hz, CH_{imz}), 7.06 (d, 1H, J = 1.8 Hz, CH_{imz}), 6.94 (d, 1H, J = 6 Hz, CH_{pyr}), 5.75 (m, 2H, C$H_{cym,\ aro}$), 5.61 (d, 1H, J = 6 Hz C$H_{cym,\ aro}$), 5.52 (d, 1H, J = 6 Hz C$H_{cym,\ aro}$), 4.21 (s, 3H, CH_{3imz}), 2.32 (m, 1H, CHMe$_{2cym}$), 2.03 (s, 3H, CH_{3cym}), 1.53 (s, 15H, CH_{3Cp^*}), 0.89 ppm (m, 6H, CHMe_{2cym}),. ^{13}C{^{1}H} NMR (100 MHz, $CDCl_3$, 27 °C): δ = 192.5, 163.2, 159.1, 153.7, 147.5, 123.7, 107.6, 103.6, 103.4, 90.5, 90.3, 90.0, 87.2, 85.6, 38.4, 31.4, 23.1, 22.1, 19.3, 9.5, 8.6 ppm. HRMS (ESI, positive ion): M^+ = 792.1022 (calculated as 792.1022 for $[C_{29}H_{37}N_3Cl_2IrRu]^+$). Anal. Calc. for $C_{29}H_{37}N_3Cl_3RuIr{\cdot}CH_2Cl_2{\cdot}0.5H_2O$: C, 39.11; H, 4.38; N, 4.56. Found: C, 39.10; H, 4.36; N, 3.83%.

Acknowledgements

J.C. sincerely thanks DAE, BRNS (Young Scientist Research Award grant no. 2011/20/37C/14/BRNS/1728), DST (Fast Track research grant No. SR/FT/CS-49/2011) and IISER Bhopal for financial support. Doctoral fellowships from CSIR (to M.M. and S.K.G.) and UGC (to R.T.K.) are gratefully acknowledged. We thank the reviewers for their insightful comments.

Notes and references

1 (*a*) K. Umehara, S. Kuwata and T. Ikariya, *J. Am. Chem. Soc.*, 2013, **135**, 6754–6757; (*b*) R. H. Crabtree, *New J. Chem.*, 2011, **35**, 18–23; (*c*) K. Muñiz, *Angew. Chem., Int. Ed.*, 2005, **44**, 6622–6627; (*d*) N. Kumagai and M. Shibasaki, *Angew. Chem., Int. Ed.*, 2013, **52**, 223–234; (*e*) J. H. Barnard, C. Wang, N. G. Berry and J. Xiao, *Chem. Sci.*, 2013, **4**, 1234–1244; (*f*) P. Cui, S. Seo, J. Lee, L. Wang, E. Lee, M. Min and H. Lee, *ACS Nano*, 2011, **5**, 6826–6833.

2 For reviews, see: (*a*) M. Melaimi, M. Soleilhavoup and G. Bertrand, *Angew. Chem., Int. Ed.*, 2010, **49**, 8810–8849; (*b*) M. Poyatos, J. A. Mata and E. Peris, *Chem. Rev.*, 2009, **109**, 3677–3707; (*c*) R. Corberán, E. Mas-Marzá and E. Peris, *Eur. J. Inorg. Chem.*, 2009, 1700–1716; (*d*) F. E. Hahn and M. C. Jahnke, *Angew. Chem., Int. Ed.*, 2008, **47**, 3122–3172; (*e*) O. Kaufhold and F. E. Hahn, *Angew. Chem., Int. Ed.*, 2008, **47**, 4057–4061; (*f*) S. Díez-González, N. Marion and S. P. Nolan, *Chem. Rev.*, 2009, **109**, 3612–3676; (*g*) H. Clavier, K. Grela, A. Kirschning, M. Mauduit and S. P. Nolan, *Angew. Chem., Int. Ed.*, 2007, **46**, 6786–6801; (*h*) K. A. Williams, A. J. Boydston and C. W. Bielawski, *Chem. Soc. Rev.*, 2007, **36**, 729–744; (*i*) W. A. Herrmann, *Angew. Chem., Int. Ed.*, 2002, **41**, 1290–1309.

3 (*a*) S. Sabater, J. A. Mata and E. Peris, *Organometallics*, 2012, **31**, 6450–6456; (*b*) S. Gonell, M. Poyatos, J. A. Mata and E. Peris, *Organometallics*, 2012, **31**, 5606–5614; (*c*) A. Zanardi, J. A. Mata and E. Peris, *J. Am. Chem. Soc.*, 2009, **131**, 14531–14537; (*d*) E. Mas-Marzá, J. A. Mata and E. Peris, *Angew. Chem., Int. Ed.*, 2007, **46**, 3729–3731.

4 (*a*) A. J. Boydston and C. W. Bielawski, *Dalton Trans.*, 2006, 4073–4077; (*b*) D. M. Khramov, A. J. Boydston and C. W. Bielawski, *Angew. Chem., Int. Ed.*, 2006, **45**, 6186–6189; (*c*) Z. Guo, N. R. Song, J. H. Moon, M. Kim, E. J. Jun,

J. Choi, J. Y. Lee, C. W. Bielawski, J. L. Sessler and J. Yoon, *J. Am. Chem. Soc.*, 2012, **134**, 17846–17849; (*d*) A. J. Boydston, P. D. Vu, O. L. Dykhno, V. Chang, A. R. Wyatt II., A. S. Stockett, E. T. Ritschdorff, J. B. Shear and C. W. Bielawski, *J. Am. Chem. Soc.*, 2008, **130**, 3143–3156; (*e*) A. G. Tennyson, E. L. Rosen, M. S. Collins, V. M. Lynch and C. W. Bielawski, *Inorg. Chem.*, 2009, **48**, 6924–6933; (*f*) K. A. Wiliams and C. W. Bielawski, *Chem. Commun.*, 2010, **46**, 5166–5168; (*g*) A. J. Boydston, J. D. Rice, M. D. Sanderson, O. L. Dykhno and C. W. Bielawski, *Organometallics*, 2006, **25**, 6087–6098.

5 (*a*) L. Benhamou, V. César, H. Gornitzka, N. Lugan and G. Lavigne, *Chem. Commun.*, 2009, 4720–4722; (*b*) L. Benhamou, N. Vujkovic, V. César, H. Gornitzka, N. Lugan and G. Lavigne, *Organometallics*, 2010, **29**, 2616–2630; (*c*) A. T. Biju, K. Hirano, R. Fröhlich and F. Glorius, *Chem. – Asian J.*, 2009, **4**, 1786–1789; (*d*) B. M. Neilson, V. M. Lynch and C. W. Bielawski, *Angew. Chem., Int. Ed.*, 2011, **50**, 10322–10326; (*e*) E. L. Rosen, C. D. Varnado Jr., A. G. Tennyson, D. M. Khramov, J. W. Kamplain, D. H. Sung, P. T. Cresswell, V. M. Lynch and C. W. Bielawski, *Organometallics*, 2009, **28**, 6695–6706; (*f*) D. M. Khramov, E. L. Rosen, V. M. Lynch and C. W. Bielawski, *Angew. Chem., Int. Ed.*, 2008, **47**, 2267–2270; (*g*) N. Vujkovic, V. César, N. Lugan and G. Lavigne, *Chem. – Eur. J.*, 2011, **17**, 13151–13155.

6 (*a*) B. M. Neilson and C. W. Bielawski, *J. Am. Chem. Soc.*, 2012, **134**, 12693–12699; (*b*) B. M. Neilson and C. W. Bielawski, *Organometallics*, 2013, **32**, 3121–3128; (*c*) B. M. Neilson and C. W. Bielawski, *Chem. Commun.*, 2013, **49**, 5453–5455; (*d*) B. M. Neilson and C. W. Bielawski, *ACS Catal.*, 2013, **3**, 1874–1885; (*e*) M. Süβner and H. Plenio, *Angew. Chem., Int. Ed.*, 2005, **44**, 6885–6888; (*f*) A. G. Tennyson, V. M. Lynch and C. W. Bielawski, *J. Am. Chem. Soc.*, 2010, **132**, 9420–9429; (*g*) S. L. Balof, B. Yu, A. B. Lowe, Y. Ling, Y. Zhang and H.-J. Schanz, *Eur. J. Inorg. Chem.*, 2009, 1717–1722.

7 For representative non-symmetric NHC ligands see: (*a*) C. Segarra, E. Mas-Marzá, M. Benítez, J. A. Mata and E. Peris, *Angew. Chem., Int. Ed.*, 2012, **51**, 10841–10845; (*b*) R. Lalrempuia, H. Müller-Bunz and M. Albrecht, *Angew. Chem., Int. Ed.*, 2011, **50**, 9969–9972; (*c*) A. McSkimming, G. E. Ball, M. M. Bhadbhade and S. B. Colbran, *Inorg. Chem.*, 2012, **51**, 2191–2203; (*d*) A. C. Badaj and G. G. Lavoie, *Organometallics*, 2012, **31**, 1103–1111; (*e*) S. Dastgir, K. S. Coleman, A. R. Cowley and M. L. H. Green, *Organometallics*, 2006, **25**, 300–306; (*f*) C. Segarra, E. Mas-Marzá, J. Mata and E. Peris, *Organometallics*, 2012, **31**, 5169–5176; (*g*) A. McSkimming, M. M. Bhadbhade and S. B. Colbran, *Dalton Trans.*, 2010, **39**, 10581–10584.

8 Selected crystallographic data for **3** and **4** are provided in the ESI.† Full crystallographic data for **3** (CCDC 945722) and **4** (CCDC 945723).

9 (*a*) E. K. van den Beuken and B. L. Feringa, *Tetrahedron*, 1998, **54**, 12985–13011; (*b*) A. Zanardi, R. Corberán, J. A. Mata and E. Peris, *Organometallics*, 2008, **27**, 3570–3576.

10 By comparing the ^{1}H NMR chemical shift values of Ru(*p*-cym)Cl_2(PPh_3) in $CDCl_3$ with the same as reported earlier in: E. Hodson and S. J. Simpson, *Polyhedron*, 2004, **23**, 2695–2707. HRMS (ESI, positive ion): M^+ = 533.0802 (calculated as 533.0771 for $[C_{28}H_{29}PClRu]^+$).

11 R. G. Ball, W. A. G. Graham, D. M. Heinekey, J. K. Hoyano, A. D. McMaster, B. M. Mattson and S. T. Michel, *Inorg. Chem.*, 1990, **29**, 2023–2025.

12 G. T. Giuffredi, S. Purser, M. Sawicki, A. L. Thompson and V. Gouverneur, *Tetrahedron: Asymmetry*, 2009, **20**, 910–920.

13 M. Rubio, E. Jellema, M. A. Siegler, A. L. Spek, J. N. H. Reek and B. de Bruin, *Dalton Trans.*, 2009, 8970–8976.

14 A. A. D. Tulloch, A. A. Danopoulos, S. Winston, S. Kleinhenz and G. Eastham, *J. Chem. Soc., Dalton Trans.*, 2000, 4499–4506.

